Use of hydrogel scaffolds to develop an in vitro 3D culture model of human intestinal epithelium

DOSH, Rasha, ESSA, A, JORDAN-MAHY, Nikki <http://orcid.org/0000-0001-8617-2636>, SAMMON, Chris <http://orcid.org/0000-0003-1714-1726> and LE MAITRE, Christine <http://orcid.org/0000-0003-4489-7107>

Use of hydrogel scaffolds to develop an *in vitro* 3D culture model of human intestinal epithelium.

R.H. Dosh [a,c], A. Essa [b], N. Jordan- Mahy [a], C. Sammon[b], C.L. Le Maitre [a,*]

[a] Biomolecular Sciences Research Centre, Sheffield Hallam University, S1 1WB, UK

[b] Materials and Engineering Research Institute, Sheffield Hallam University, S1 1WB, UK

[c] Department of Anatomy and Histology, University of Kufa, Kufa, Iraq

E-mail addresses:

Dosh RH: rasha.h.dosh@student.shu.ac.uk

A. Essa: b4034845@my.shu.ac.uk

Jordan-Mahy N: n.jordan-mahy@shu.ac.uk

Sammon C: c.sammon@shu.ac.uk

*Corresponding author: Prof. Christine Lyn Le Maitre, Biomolecular Science Research Centre, Sheffield Hallam University, S1 1WB, UK.

Email**:** c.lemaitre@shu.ac.uk

Phone +44 (0)114 225 6613 Fax +44 (0)114 225 3064

Abstract

The human intestinal cell lines: Caco-2 and HT29-MTX cells have been used extensively in 2D and 3D cell cultures as simple models of the small intestinal epithelium *in vitro*. This study aimed to investigate the potential of three hydrogel scaffolds to support the 3D culture of Caco-2 and HT29-MTX cells and critically assess their use as scaffolds to stimulate villi formation to model a small intestinal epithelium *in vitro*. Here, alginate, L-pNIPAM, and L-pNIPAM-co-DMAc hydrogels were investigated. The cells were suspended within or layered on these hydrogels and maintained under static or dynamic culture conditions for up to 21 days. Caco-2 cell viability was increased when layered on the synthetic hydrogel scaffolds, but reduced when suspended within the synthetic hydrogels. In contrast, HT29-MTX cells remained viable when suspended within or layered on all 3D cultures. Interestingly, cells cultured in and on the alginate hydrogel scaffolds formed multilayer spheroid structures, whilst the cells layered on synthetic hydrogels formed villus-like structures. Immunohistochemistry staining demonstrated positive expression of enterocyte differentiation markers and goblet cell marker. In conclusion, L-pNIPAM hydrogel scaffolds supported both cell lines and induced formation of villus-like structures when cells were layered on and cultured under dynamic conditions. The ability of the L-pNIPAM to recapitulate the 3D structure and differentiate main cell types of human intestinal villi may deliver a potential alternative *in vitro* model for studying intestinal disease and for drug testing.

Keywords: Caco-2 cells, HT29-MTX cells, alginate, L-pNIPAM, L-pNIPAM-co-DMAc

Abbreviations:

ISEMF: Intestinal subepithelial myofibroblast; PLGA: Poly Lactic-co-Glycolic Acid; NIPAM: N-isopropylacrylamide; AIBN: 2-2'-azobisisobutyronitrile; LCST: lower critical solution temperature; DMA: dynamic mechanical analysis; DMAc: N, N' – dimethylacrylamide; SEM: scanning electron microscopy; i.d: internal dimension; IHC: Immunohistochemistry; ZO-1: zonulin-1; ALP: alkaline phosphatase; DPP IV: dipeptidyl peptidase 4; SI: sucrase-isomaltase. L-pNIPAM: hydrogel composed of 9% NIPAM, 1% Laponite® and 90% water (by weight); L-pNIPAM-co-DMAc: hydrogel composed of 7.83% NIPAM, 1.17% DMAc, 1% Laponite® and 90% water (by weight)(see methods).

1. Introduction

In vitro 3D intestinal models are becoming useful tools for investigating how human intestinal cells function and are regulated [1]. The studies of intestinal cellular proliferation, migration, differentiation, and drug absorption using *in vivo* models have limitations. These include difficulties in controlling the cell behaviour, their responses to specific environmental prompts, and the way in which they absorb compounds [1,2]. Hence, this has led to the development of a number of 3D *in vitro* intestinal models. It is suggested that these 3D models could be useful to investigate tissue engineering, drug discovery, and used as an alternative to *in vivo* animal models in drug toxicity studies [3–5]. Previously, *in vitro* intestinal models have been limited to 2D cell culture [6,7], however, a number of studies have attempted to develop 3D intestinal models *in vitro* to mimic the morphological characteristics and function of intestinal epithelial cells to represent the micro-environment seen *in vivo* [2,8,9]. The choice of cells within the models is a major challenge due to the restricted accessibility to obtain sufficient quantity of primary cells which are required for 3D *in vitro* intestinal models [10].

To date, a number of normal and tumour cell types have been tested for their ability to generate intestinal epithelial models. When rat intestinal epithelial cell line (IEC-6) were seeded on top of rat intestinal subepithelial myofibroblasts (ISEMF) embedded in a collagen gel, the ISEMF were shown to induce differentiation of the overlying IEC-6 cells into enteroendocrine cells after 3 weeks [11]. Viney *et al,* (2010) co-cultured IEC-6, IPI-21 (small boar ileum epithelial cell line), and CRL-2102 (human epithelial cell line derived from colorectal adenocarcinoma) with Rat-2 (fibroblast-like cells) on collagen gel alone or on a collagen-Matrigel scaffold. They demonstrated that the greatest epithelial growth was seen on collagen gels supplemented with

Matrigel after 20 days, where they observed multi-layered intestinal epithelium containing a cluster of cells resembling native small intestinal crypts [12].

To reduce the cost and ethical concerns raised by using *in vivo* animal models, Caco-2 and HT29-MTX human colon adenocarcinoma cell lines have been extensively employed in *in vitro* models. These cells have been selected due to their capacity to differentiate into enterocyte-like cells and mucus-producing goblet cells respectively, plus they demonstrated properties which are characteristic of the small intestine *in vitro* [13]. In 2D culture, Caco-2 cells form a monolayer, and spontaneously differentiate when confluent, expressing morphological and functional characteristics of enterocytes. These cells display polarized morphology, with microvilli on the apical side, tight junctions between the adjacent cells and express high levels of hydrolase enzymes such as alkaline phosphatase, sucrase-isomaltase, and peptidase [14–17]. Whereas HT29-MTX cells are characterized by the development of confluent monolayers, junction formation and express high level of mucus [18].

It has been shown, that the use of 3D scaffolds can drive cell proliferation and differentiation [1,19]. However, the cell growth rate varies depending on the scaffold used. Hence, the selection of scaffolds and matrices depends on cell type and other culture conditions [3]. Previous studies have investigated a number of potential biomaterial scaffolds for the formation of 3D models of the small intestine [1,20]. Collagen gel has been widely used as a scaffold to develop a 3D model of the small intestine, although collagen gels are limited by batch variation. Most notably, Caco-2 cells have been investigated within 3D collagen scaffolds which were fabricated prior to seeding to match the geometry of intestinal villi. On these moulded collagen scaffolds, Caco-2 cells proliferated and migrated to form structures resembling

intestinal villi [1,19,21]. Sung *et al*, (2011) demonstrated that the fabricated micro-scale collagen structure mimicking the intestinal villi and could be used as a scaffold for Caco-2 cells in the investigation of drug permeability [22]. In addition, several studies have exploited biodegradable fabricated co-polymers such as poly lactic-co-glycolic acid (PLGA). These scaffold moulds have been used in co-culture studies of Caco-2 and HT29-MTX and were shown to give rise to villi-like structures [1,23]. However, to date, no realistic 3D models which form intestinal villi without prefabrication of structures prior to culture have been achieved.

Hence, this study aimed to investigate alternative hydrogels which could be used to develop a 3D model of the small intestinal villi *in vitro*. A number of hydrogels have potential in the tissue engineering of small intestinal villi. Calcium cross-linked alginate hydrogels are increasingly being used as a 3D culture system for mammalian cells in biomedical engineering studies [24,25]. Alginate is generally softer than some of the more commonly used collagen gels and enables facile diffusion of nutrients and cellular migration, which may be beneficial in the formation of villi structures. Here we investigated three hydrogels which have not been previously used in 3D culture for immortalized human intestinal epithelial cells: an alginate hydrogel; a novel synthetic non-biodegradable hydrogel systems L-pNIPAM [26,27] and L-pNIPAM-co-DMAc [28]. As these hydrogels are highly hydrated, it is hypothesized that this would support the growth of a small intestinal model, which could mimic the cellular phenotypes of the small intestine. The latter two have been developed by our group, these hydrogels can be closely controlled and due to their synthetic nature do not display batch variation which is a major disadvantage of natural materials. Furthermore as these hydrogels display an extremely low viscosity they can be moulded into any shape required and enable incorporation of cells either

pre or post gelation. Thus if these systems are shown to support intestinal cells here they could be utilised in more complex culture systems in the future, e.g. they could be used to line tubing to mimic more closely the structures seen in the intestine. Furthermore, we have previously validated that these hydrogels are cytocompatible [28]. Here, we investigated the potential of these three hydrogel systems to support the 3D culture of Caco-2 and HT29-MTX cells and determine their use as scaffolds to support formation of the villi architecture of the *in vitro* small intestine.

2. Materials and methods

2.1. Hydrogel scaffolds synthesis

2.1.1. Alginate hydrogel scaffolds

1.2% (w/v) medium viscosity of alginic acid sodium salt (Sigma-Aldrich, Poole, UK) in 0.15M NaCl (Sigma-Aldrich, Poole, UK) and filter sterilized. To prepare alginate: 300µL alginate was added to each well of 48 well plates for histological assessment and 100µL added to each well of 96 well plates for metabolic activity analysis. Alginate was carefully overlaid with 300µL in 48 well plates and 100µL in 96 well plates of 200mM $CaCl_2$ and incubated at 37°C for 10 min to induce gelation.

2.1.2. L-pNIPAM hydrogel scaffolds

Laponite® clay nanoparticles (25–30 nm diameter, ≤1 nm thickness) (0.1g) were dispersed in deionised H_2O (9.0ml) (18 mΩ) for 24 h. N-isopropyl acrylamide (BYK Additives Ltd, Cheshire, UK) was prepared by vigorous stirring of 99% NIPAM (0.9g) (Sigma, Poole, UK) and 1% 2-2'-azobisisobutyro nitrile (AIBN) (0.009g) (Sigma, Poole, UK) for 1h. After passing the suspension through a 5 – 8µm pore filter paper, the polymerization was initiated by heating to 80°C and the reagents were allowed to

158 react for 24h. It was observed that after heating the monomeric suspension to 80°C,
159 the transparent liquid transforms to a milky suspension, which is comprised of a
160 statistical co-polymer with a composition of 1% Laponite, 9% pNIPAM, and 90%
161 water (by weight) [26,27]. Following 24h the hydrogel suspension was cooled to 38 -
162 39°C prior to cell incorporation. Further cooling of the polymeric suspension to 32°C,
163 i.e. below the lower critical solution temperature (LCST) resulted in rapid gelation to
164 a solidified hydrogel.

165 **2.1.3. L-pNIPAM-co-DMAc hydrogel scaffolds**

166 L-pNIPAM-co-DMAc hydrogel was synthesized as previously described [28] Briefly,
167 0.1g Laponite® clay nanoparticles (25-30nm diameter, ≤1nm thickness) were
168 dispersed in deionised H_2O (9.0ml) (18mΩ) for 24h. N-isopropyl acrylamide (BYK
169 Additives Ltd, Cheshire, UK) was prepared by vigorous stirring 0.783g NIPAM
170 (Sigma, Poole, UK), 0.117g N,N'-dimethyl acrylamide (DMAc) (Sigma, Gillingham,
171 UK) and 0.009g 2-2'-azobisisobutyro nitrile (AIBN) (Sigma, Poole, UK) were added
172 to the suspension and stirred for 1h. After passing the suspension through a 5-8µm
173 pore filter paper, the polymerization was initiated by heating to 80°C and the
174 reagents were allowed to react for 24h. It was observed that after heating the
175 monomeric suspension to 80°C, the transparent liquid transformed to a milky
176 suspension, which is comprised of a statistical co-polymer with a composition of 1%
177 Laponite, 7.83% pNIPAM, 1.17% DMAc and 90% water (by weight). Following 24h
178 the hydrogel suspension was cooled to 38-39°C prior to cell incorporation. Further
179 cooling of the polymeric suspension to 37°C, i.e. below the LCST, resulted in rapid
180 gelation to a solidified hydrogel.

181 **2.2: Material Characterisation**

2.2.1: Scanning electron microscopy (SEM)

The morphology of all samples was investigated using a scanning electron microscope, the samples were taken as prepared and frozen at -80°C and subsequently freeze dried using (FD-1A-50) and fractured into two or more pieces to obtain a cross-sectional edges. Samples were then mounted onto aluminium stubs and gold coated using (Q150T-ES sputter coater (Quorum, UK). (10lA sputter current for 190 s with a 2.7 tooling factor).

The fractured samples were examined using (FEI NOVA nano-SEM 200 scanning electron microscope). Images were obtained using accelerating voltage 5 KV with a range of magnifications (1000 to 10,000). From images captured, six images were randomly selected for each sample at 2400 magnification and pore sizes measured using the Capture Pro OEM v8.0 software (Media Cybernetics, Buckinghamshire, UK),

2.2.2: Dynamic mechanical analysis (DMA)

Samples were either cast directly into an in-house designed sample holder for synthetic hydrogel samples or by making 3mm thick sheet at room temperature (2 h), and a circular biopsy punch (4.5mm i.d.) was used to remove cylindrical samples from the solid alginate, all samples dimensions were confirmed using digital callipers prior to measurement.

DMA was conducted in compression mode, using frequency testing type (0.063 - 10 Hz) at room temperature (PerkinElmer DMA 8000) and storage moduli determined. Six replicates for each sample were measured.

205 ## 2.3. Cell lines

206 The human immortal epithelial cell lines Caco-2, (passage 18-27), and HT29-MTX
207 cells, (passage 25-30), were obtained from the American Type Culture Collection
208 (ATCC). Cells were cultured in complete cell culture media consisting of DMEM
209 media (Life Technologies, Paisley, UK) supplemented with 20% (v/v) heat-inactivated
210 foetal calf serum (FCS) for Caco-2 cells and 10% (v/v) FCS for HT29-MTX cells (Life
211 Technologies, Paisley, UK), 100U/M penicillin (Life Technologies, Paisley, UK),
212 100µg/ml streptomycin (Life Technologies, Paisley, UK), 250ng/ml amphotericin
213 (Sigma, Poole, UK), 2mM glutamine (Life Technologies, Paisley, UK) and 1% (v/v)
214 non-essential amino acids (NEAA) (Sigma, Poole, UK). Cells were maintained in an
215 incubator at 37°C temperature and 5% CO_2 in a humid atmosphere. Culture medium
216 was replaced every 2 days. At 70-80% confluence, cells were washed with PBS (Life
217 technologies, Paisley, UK) and then treated with 0.25% w/v trypsin-EDTA (Life
218 technologies, Paisley, UK) and sub-cultured.

219 ### 2.3.1. Culture conditions

220 Caco-2 and HT29-MTX cells were seeded at a density of $2x10^6$ cells/ml either
221 suspended in or layered onto the surface of the three hydrogels (alginate, L-
222 pNIPAM, and L-pNIPAM-co-DMAc).

223 To prepare suspended cells in alginate culture: $2x10^6$ cells/ml were suspended in
224 alginate and 300µL added to each well of 48 well plates for histological assessment
225 and 100µL added to each well of 96 well plates for metabolic activity analysis.
226 Alginate was carefully overlaid with 300µL in 48 well plates and 100µL in 96 well
227 plates of 200mM $CaCl_2$ and incubated at 37°C for 10 min to induce gelation. $CaCl_2$
228 was removed and samples were washed twice in 0.15M NaCl to remove free Ca^{2+},

and complete media, before 500µL of complete culture media was added to each well of 48 well plate, and 250µL of complete media was added to each well of 96 well plates. Cells were incubated at 37°C, 5% CO_2 and maintained in culture for 14 and 21 days under static and dynamic 3D culture conditions using an orbital shaker at 30 rpm, with media replenished every 48h.

To prepare L-pNIPAM and L-pNIPAM-co-DMAc suspensions: $2x10^6$ cells/ml were suspended within either L-pNIPAM or L-pNIPAM-co-DMAc at 38-39°C. Three hundred microliters of hydrogel cell suspension was added to each well of 48 well plates and 100µL of hydrogel suspension was added to each well of 96 well plates and allowed to cool below the LCST to induce gelation. Five hundred microliters of complete culture media were added to each well of 48 well plates and 250µL of complete culture media was added to each well of 96 well plates. Cells were then incubated at 37°C, 5% CO_2 and maintained in culture for 14 and 21 days under static and dynamic 3D culture conditions using an orbital shaker at 30 rpm. With media replenished every 48h.

To prepare layered cultures, 300µL of either alginate, L-pNIPAM or L-pNIPAM-co-DMAc were added to each well of 48 well plates and 100µL added to each well of 96 well plates. Alginate culture gelation was induced by application of $CaCl_2$, whilst gelation of the L-pNIPAM and L-pNIPAM-co-DMAc was induced by cooling. Following gelation 300µL or 100µL of $2x10^6$ cells/ml in complete media were applied to the surface of each hydrogel construct in 48 and 96 well plates, respectively and a further 200µL or 150µL complete media added to each well after 30min cell attachment period. All constructs were incubated at 37°C, 5% CO_2 and maintained in culture for 14 and 21 days under static and dynamic 3D culture conditions using an orbital shaker at 30 rpm, with media replenished every 48h.

2.4. Cytospins of monolayer control cells

Monolayer cells were fixed in 4% w/v paraformaldehyde (Sigma, Poole, UK) for 20min. To generate a cell pellet, cells spun at 300g for 5min and suspended in PBS to a cell density of 300 cell/µl. One hundred microliters of cell suspension was cytospun by centrifugation at 1000 rpm for 3min (Shandon cytospin 3, Thermo Scientific, Loughborough, UK). Slides were then air-dried and stored at 4°C until needed for immunohistochemical investigation.

2.5. Metabolic activity of cells

The metabolic activity of Caco-2 and HT29-MTX cells suspended within and layered on hydrogels under static and dynamic 3D culture conditions were assessed using Alamar blue assay (Life Technologies, Paisley, UK) in normal complete media after 0-21 days of culture following the manufacturer's protocol. The fluorescent intensity was recorded using a fluorescence microplate reader (CLARIOstar®, BMG LABTECH) fluorescence excitation wavelength of 590nm. Relative fluorescence units (RFU) were recorded for cellular hydrogel scaffolds and normalized to RFU of acellular control scaffolds as an indication of total live cells.

2.6. Histological assessment

Caco-2 and HT29-MTX cells were cultured suspended within or layered on each of the three hydrogel scaffolds, under static or dynamic culture conditions, together with no cell controls for 14 and 21 days. Triplicate samples were fixed in 4% w/v paraformaldehyde/PBS for 24h prior to washing in PBS and processed to paraffin wax in a TP1020 tissue processor (Leica Microsystem, Milton Keynes, UK). Four-micron sections were cut and mounted onto positively charged slides (Leica Microsystem Milton Keynes, UK). Sections were deparaffinised in Sub-X and

rehydrated in industrial methylated spirits (IMS) prior to rehydration in distilled water. Sections were then stained with either: Haematoxylin and Eosin; Mayer's Haematoxylin (Leica Microsystem, Milton Keynes, UK) for 2 min rinsed in water for 5 min and immersed in Eosin (Leica Microsystem, Milton Keynes, UK) for 1 min); or Alcian Blue/Periodic acid Schiff's (PAS): 1% w/v Alcian Blue (PH 2.5) (Sigma-Aldrich, Poole, UK) in 3% (v/v) acetic acid (Sigma-Aldrich, Poole, UK) for 30 min and immersed in 0.5% (w/v) Periodic acid for 10 min and rinsed three times in deionized water. Slides were then immersed in Schiff reagent (Merck KGaA, Germany) for 10 min, then rinsed three times with deionized water. Following staining, sections were dehydrated in IMS, cleared with Sub-X and mounted in Pertex (Leica Microsystem, Milton Keynes, UK). The slides were examined with an Olympus BX 51 microscope and images captured by the camera and Capture Pro OEM v8.0 software (Media Cybernetics, Buckinghamshire, UK).

2.7. Immunohistochemical Assessment

Immunohistochemistry was performed on Caco-2 and HT29-MTX cells harvested from monolayer cultures (cytospins) prior to hydrogel incorporation to serve as time zero controls. Together with cells cultured on the optimal hydrogel culture conditions for 21 days in culture. Immunohistochemistry was performed to investigate: brush border differentiation using CD10 antibody (1:100 rabbit polyclonal, enzyme antigen retrieval) (Abcam, Cambridge, UK); Zonulin 1 (ZO-1) protein expression which is a tight junction protein expressed by enterocytes using ZO-1 antibody (1:50, enzyme antigen retrieval) (Abcam, Cambridge, UK); enterocyte differentiation markers: alkaline phosphatase (ALP) antibody (1:200 rabbit polyclonal, heat antigen retrieval) (Abcam, Cambridge, UK), dipeptidyl peptidase IV (DPP IV) antibody (1:50 mouse monoclonal, enzyme antigen retrieval) (Abcam, Cambridge, UK); and sucrase-

isomaltase antibody (SI) (1:50, mouse monoclonal antibody, heat antigen retrieval) (Santa Cruz, Heidelberg, Germany); HT29-MTX differentiation was assessed using MUC2 antibody (1:100 rabbit polyclonal, heat antigen retrieval) (Santa Cruz, Heidelberg, Germany) and MUC5AC antibody (1:200, mouse monoclonal antibody, heat antigen retrieval) (Abcam, Cambridge, UK).

Immunohistochemistry was performed as previously described [29]. Briefly, 4µm sections were de-waxed, rehydrated, and endogenous peroxidase blocked using hydrogen peroxide (Sigma-Aldrich, Poole UK). After washing in tris-buffered saline (TBS) (20 mM tris, 150 mM sodium chloride, pH 7.5), sections were subjected to antigen retrieval methods. Following TBS washing, nonspecific binding sites were blocked at room temperature for 90 min with 25% (w/v) serum (Abcam, Cambridge, UK) in 1% (w/v) bovine serum albumin in TBS. Sections were incubated overnight at 4°C with appropriate primary antibody. Negative controls in which rabbit and mouse IgGs (Abcam, Cambridge, UK) replaced the primary antibody at an equal IgG concentration were used. Sections were washed in TBS and then incubated in 1:500 dilution of appropriate biotinylated secondary antibody for 30min at room temperature. Binding of the secondary antibody was disclosed by horseradish peroxidase (HRP) streptavidin-biotin complex (Vector Laboratories, Peterborough, UK) for 30min. Sections were washed in TBS, and treated with 0.08% (v/v) hydrogen peroxide in 0.65mg/ml 3, 3′-diaminobenzidine tetrahydrochloride (Sigma-Aldrich, Poole, UK) in TBS for 20min. Sections were counterstained with Mayer's haematoxylin, dehydrated, cleared and mounted in Pertex. The slides were examined with an Olympus BX51 microscope and images captured by the camera and Capture Pro OEM v8.0 software (Media Cybernetics, Buckinghamshire, UK).

2.8. Scanning electron microscopy following cell culture

After 21 days in culture, samples were processed for scanning electron microscopy (SEM). Briefly, the samples were removed from the culture, frozen at -80°C then freeze dried overnight using a FD-1A-50 freeze dryer (Genorise Scientific). The samples were then fractured to expose the interior surface morphology. The fractured samples were mounted on aluminum stubs and coated with gold using a Quorum Technology 150Q TES system set at 10µA sputter current for 180s with a 2.7 tooling factor. The cells were examined using a FEI NOVA nano-200 scanning electron microscope.

2.9. Statistical analysis

All viability tests were performed at least 6 times. Normality was assessed using Stats Direct with the normality tests. This utilises multiple normality tests (Skewness, Kurtosis, Royston Chi-sq, Shapiro Wilk W and Shapiro-Francia W, together with a q-q plot). From this analysis it was demonstrated that the data sets were from mixed populations with some populations displaying potential normal distribution but others were shown to be not normally distributed, as such non-parametric tests have been performed for all data. Therefore statistical comparisons were performed by Kruskal-Wallis with a pairwise comparison (Dwass-Steel-Critchlow-Fligner) between all-time points and between culture conditions and hydrogel systems for 21 days for Alamar blue assay with statistical significance accepted at $P \leq 0.05$.

3. Results

3.1 Material properties of Alginate, L-pNIPAM and L-pNIPAM-co-DMAc scaffolds.

Alginate displayed significantly larger pores (30-74µm) and lowest storage moduli (0.4-8.6x10^5 Pa) than both the synthetic hydrogels investigated (Supplementary Fig.

1A & B). L-pNIPAM displayed significantly larger pores (5.6-25µm) and lower storage moduli (0.18-2.8x10^7 Pa) than L-pNIPAM-co-DMAc (Supplementary Fig. 1A & B). L-pNIPAM-co-DMAc displayed the smallest pore sizes (1.5-30µm) and highest storage moduli (1-5x10^7 Pa) indicating this was the stiffest of the three hydrogels investigated (Supplementary Fig. 1A & B).

3.2. Metabolic activity of Caco-2 cells in three hydrogel scaffolds

3.2.1. Alginate hydrogel scaffold

Under static layered culture conditions, there was a significant decrease in cell metabolic activity of Caco-2 cells between day 0 and 2, when grown on alginate ($P \leq 0.05$) (Fig. 1A). Thereafter metabolic activity was significantly increased between day 2 to 14 ($P \leq 0.05$) (Fig. 1A). Likewise, when Caco-2 cells were suspended in alginate and cultured under static conditions, there was a decreased metabolic activity from day 0 and 7, which was then followed by a significant increase in metabolic cell activity from day 2 and day 7 to day 14 and 21 ($P \leq 0.05$) (Fig. 1B). In contrast, under dynamic culture conditions, there was an increase in metabolic cell activity in Caco2 cells between day 0 and 7 when layered on the alginate, followed by a decrease in metabolic cell activity from day 7 to 21 which failed to reach significance (Fig. 1C). No significant difference in metabolic cell activity during the initial 7 days of culture when the Caco-2 cells were suspended within alginate, this was then followed by a significant increase in metabolic cell activity from day 7 to 21 under dynamic culture ($P \leq 0.05$) (Fig. 1D). Across the culture conditions following 3 weeks a significant decrease in metabolic activity was observed in Caco-2 cells layered on the surface of alginate cultured under dynamic conditions compared to static conditions ($P \leq 0.05$)(Fig.1A-1C). Whilst cells cultured under dynamic culture in

suspension showed an increase in metabolic activity compared to layered cultures under dynamic conditions (P≤0.05)(Fig. 1C-1D).

3.2.2. L-pNIPAM hydrogel scaffold

When Caco2 cells were cultured as layers on the surface of L-pNIPAM hydrogel scaffolds under either static or dynamic culture, there was no change in metabolic cell activity from day 0 to 2. This was followed by a significant increase in metabolic cell activity from day 7 to 21 (P≤0.05) (Fig.1E & G). In contrast, when Caco-2 cells were suspended in L-pNIPAM and cultured under either static or dynamic conditions there was a significant decrease in metabolic cell activity (P≤0.05) (Fig. 1F & H). Across the culture conditions following 3 weeks a significant decrease in metabolic activity was seen in Caco-2 cells suspended in L-pNIPAM compared to layered cells under both static and dynamic culture (P≤0.05)(Fig. 1E-1H).

3.2.3. L-pNIPAM-co-DMAc hydrogel scaffold

Under both static and dynamic culture conditions, there was a significant increase in metabolic cell activity from day 0 when Caco-2 cells were layered on the L-pNIPAM-co-DMAc (P≤0.05) (Fig. 1I & K). However, when Caco-2 cells were suspended within L-pNIPAM-co-DMAc there was a significant decrease in metabolic cell activity, under both static and dynamic cultures conditions (P≤0.05) (Fig. 1J & L). Across the culture conditions following 3 weeks a significant decrease in metabolic activity was seen in Caco-2 cells suspended in L-pNIPAM-co-DMAc compared to layered cells under both static and dynamic culture (P≤0.05)(Fig. 1I-1L).

3.2.4. Comparison of metabolic activity between three hydrogel systems.

Caco-2 cells cultured under static conditions in layers displayed no significant difference in metabolic activity following 3 weeks (Fig. 1). Whilst Caco-2 cells

cultured in suspension either under static or dynamic culture showed significantly higher metabolic activity in alginate culture compared to both L-pNIPAM and L-pNIPAM-co-DMAc following 3 weeks ($P<0.05$)(Fig.1). In contrast, Caco-2 cells cultured in layers in dynamic culture showed highest metabolic activity in L-pNIPAM which was significantly higher than both L-pNIPAM-co-DMAc and alginate cultures following 3 weeks ($P<0.05$)(Fig.1). Furthermore, metabolic activity of Caco-2 cells cultured in layers on L-pNIPAM-co-DMAc under dynamic culture was significantly higher than cells cultured on alginate following 3 weeks ($P<0.05$)(Fig.1).

3.3. Morphological and phenotypic assessment of Caco-2 cells cultured in hydrogel systems

Caco-2 cells cultured in layers on alginate under either static or dynamic culture commonly formed multilayer spheroid structures (Fig. 2A). When cells were suspended within alginate they formed large cell clusters which had clearly defined nuclei by day 14 to 21 (Fig. 2A and Supplementary Fig. 2A). In contrast Caco-2 cells cultured as layers on the surface of L-pNIPAM under static culture conditions formed small multicellular layers, parallel to the surface of the hydrogel between day 14 and 21 (Fig. 2A and Supplementary Fig. 2A). However, when Caco-2 cells were grown as layers on the surface of L-pNIPAM under dynamic culture conditions, these cells were found to migrate into the hydrogel by day 14 (Supplementary Fig. 2A) and then give rise to villus-like structures by day 21 (Fig. 2A).

However, when Caco-2 cells were suspended in L-pNIPAM and maintained under either static or dynamic culture conditions cells showed poor nuclear morphology, consistent with non-viable cells (Fig. 2A). Similarly, when Caco-2 cells were suspended within L-pNIPAM-co-DMAc and maintained under both static and

dynamic culture, cells only formed a few small clusters of cells between day 14 and 21. In contrast, Caco-2 cells grown as layers on the surface of L-pNIPAM-co-DMAc under static and dynamic conditions formed multi-cellular layers and villus-like structures (Fig. 2A and Supplementary Fig. 2A).

To determine potential mucin production, samples were stained using alcian blue/PAS. Whilst all three hydrogels showed background staining for alcian blue, cellular structures within them could be easily distinguished, however due to the high levels of background staining for acidic mucins within all hydrogels, no increased staining over background was observed for acidic mucins. Within alginate scaffolds, cells were positive for neutral (pink) mucins in all culture conditions (Fig. 2B and Supplementary Fig. 2B). Immunohistochemical analysis of MUC2 and MUC5AC showed Caco-2 cells did not express MUC2 and MUC5AC mucins in monolayer culture (0 hr cytospin), or in cells cultured as layers or suspended in all three hydrogels under either static or dynamic culture (Supplementary Fig. 3A, B, and C).

From this analysis, L-pNIPAM was selected for further phenotypically analysis due to the superior morphological appearance and mucin production. To determine the level of Caco-2 cellular differentiation, the expression of three brush border enzymes, together with enterocyte brush border marker and a tight junction protein were investigated. Immunopositivity for CD10, ZO-1, ALP, DPP IV and SI were seen in monolayer cultures (0 hr cytospin) and on the cell surface of all Caco-2 cells layered on L-pNIPAM maintained under either static or dynamic culture (Fig. 3).

3.4. Scanning electron microscopy of Caco-2 cells

SEM analysis of Caco-2 cell cultures in layers on the surface of L-pNIPAM and L-pNIPAM-co-DMAc hydrogel scaffolds was performed (Fig. 4A & B). Under static and

dynamic culture conditions Caco-2 cells layered on L-pNIPAM formed comprehensive multi-layer clusters of cells which often gave rise to villi-like structures by day 21 (Fig. 4A and Supplementary Fig. 5). Close examination of the edges of these cell clusters showed the presence of microvilli brush borders. Surprisingly, layered Caco-2 cells when spread on the surface of L-pNIPAM-co-DMAc under static and dynamic culture conditions, covered the entire surface of the scaffold (Fig. 4B and Supplementary Fig. 5). As can be seen no cell controls which were cultured in media for the same 3 week duration do not display any of these cellular like structures demonstrating these features are specific to those hydrogels containing cells (Fig. 4).

3.5. Metabolic activity of HT29-MTX cells in three hydrogel scaffolds

3.5.1. Alginate hydrogel scaffold

Under static culture conditions, a significant increase in metabolic cell activity was observed between 0 and 21 days when HT29-MTX cells were layered on alginate ($P \leq 0.05$) (Fig. 5A). However, when HT29-MTX cells were suspended within alginate, a significant decrease in metabolic cell activity between day 0 and 21 ($P \leq 0.05$) (Fig. 5B). In contrast, under dynamic culture conditions, there was a significant increase in metabolic cell activity between day 0 and 7, 14 and 21, when HT29-MTX cells were layered on alginate ($P \leq 0.05$) (Fig. 5C). Whereas HT29-MTX cells when suspended within alginate showed a significant decrease in metabolic cell activity between day 0 and 2, which was followed by a significant increase in metabolic cell activity at day 21 ($P \leq 0.05$) (Fig. 5D). Across the culture conditions following 3 weeks a significant decrease in metabolic activity was observed in HT29-MTX cells suspended compared to those layered on the surface and cultured under static conditions

(P≤0.05) (Fig. 5A-1B). Whilst cells cultured under dynamic layered culture showed an increase in metabolic activity when compared to static layered conditions (P≤0.05) (Fig. 5A-1C).

3.5.2. L-pNIPAM hydrogel scaffold

Under static culture conditions, when HT29-MTX cells were layered on or suspended in L-pNIPAM there was a significant decrease in metabolic cell activity observed between day 0 and 2, followed by a significant increase in metabolic cell activity between day 7 and 21 (P≤0.05) (Fig. 5E and 5F). Under dynamic culture conditions, initially there was a significant decrease in metabolic cell activity detected from 0 to 2 days (P≤0.05); followed by a significant increase in metabolic cell activity from day 2 to 21 (P≤0.05) (Fig. 5G & 5H). Across the culture conditions following 3 weeks a significant difference in metabolic activity was seen in HT29-MTX cells suspended in L-pNIPAM compared to layered cells under both static and dynamic culture (P≤0.05) (Fig. 5E-5H).

3.5.3. L-pNIPAM-co-DMAc hydrogel scaffold

Under static culture conditions, a significant increase in metabolic cell activity was observed at all time points where HT29-MTX cells were layered on L-pNIPAM-co-DMAc (P≤0.05) (Fig. 5I). In contrast, a significant increase in metabolic cell activity was observed from day 2 to 7 followed by a significant decrease in metabolic cell activity from day 7 to 21 when HT29-MTX cells were suspended in L-pNIPAM-co-DMAc (P≤0.05) (Fig. 5J). Under dynamic culture conditions, when HT29-MTX cells were layered on L-pNIPAM-co-DMAc there was a significant increase in metabolic cell activity from day 0 to 7 (P≤0.05) (Fig. 5K). Whereas, when HT29-MTX cells were suspended within L-pNIPAM-co-DMAc and maintained under dynamic culture

conditions, there was a significant increase in metabolic cell activity following 14 days in culture (P≤0.05) (Fig. 5L). Across the culture conditions following 3 weeks a HT29-MTX cells displayed significantly higher metabolic activity when cultured layered in static conditions compared to suspended in L-pNIPAM-co-DMAc under static conditions or layered under dynamic conditions (P≤0.05) (Fig. 5I-5L).

3.5.4. Comparison of metabolic activity between three hydrogel systems.

HT29-MTX cells cultured under static conditions in layers displayed no significant difference in metabolic activity following 3 weeks (Fig. 5). Whilst HT29-MTX cells cultured in suspension either under static or dynamic culture showed significantly higher metabolic activity in L-pNIPAM compared to both alginate and L-pNIPAM-co-DMAc following 3 weeks (P<0.05) (Fig.5). In contrast, HT29-MTX cells cultured in layers in dynamic culture showed highest metabolic activity in alginate which was significantly higher than both L-pNIPAM and L-pNIPAM-co-DMAc cultures following 3 weeks (P<0.05) (Fig.5).

3.6. Morphological and phenotypic assessment of HT29-MTX cells cultured in hydrogel systems

HT29-MTX cells cultured in layers on alginate under either static or dynamic culture conditions formed multilayer spheroids following 14 days (Supplementary Fig. 4A), which continuously enlarged over the 21 days of culture (Fig. 6A). However, multilayers of HT29-MTX cells were observed when cells were layered on alginate hydrogel scaffolds under static and dynamic culture at day 21 (Supplementary Fig. 3A and Fig. 6A). In contrast, HT29-MTX cells layered on L-pNIPAM under static and dynamic culture conditions at day 14 and 21, accumulated as multilayers of cells and formed villus-like structures. This differed considerably to suspended HT29-MTX

cells, which migrated to the surface of L-pNIPAM and formed a multilayer of cells under static conditions propagating the formation of villus-like structures under dynamic conditions (Supplementary Fig. 4A and Fig. 6A). As a result by day 21, well-developed mucosal-like layers formed when HT29-MTX cells were layered on and suspended in L-pNIPAM-co-DMAc under both static and dynamic culture conditions (Supplementary Fig. 4A and Fig. 6A).

HT29-MTX cells grown for 21 days on and in the three hydrogel systems under dynamic and static culture differentiated to form mucus-producing goblet-like cells, (Supplementary Fig. 4B and Fig. 6B). Whilst background staining for acidic mucins was again high in no cell controls, clear increases in intensity for acidic mucins were observed around cells in all cultures of HT29-MTX cells (Fig. 6). Although acidic and neutral mucins were secreted by the HT29-MTX cells in all cultures the secretion patterns varied. In alginate, acidic and neutral mucins were secreted in all culture conditions at day 14 and 21 (Supplementary Fig. 4B and Fig. 6B). Increased secretion of acidic mucins over neutral mucins were observed in L-pNIPAM hydrogel scaffolds, additionally mucus covered the HT29-MTX cells by day 21, in all culture conditions. Although the secretion of acidic mucin was observed in HT29-MTX cells layered on and suspended in L-pNIPAM-co-DMAc, neutral mucins were also detected after day 21, under both static and dynamic culture (Supplementary Fig. 4B and Fig. 6B).

Immunopositivity for MUC2 and MUC5AC was observed in control cytospun HT29-MTX cells grown in monolayer. Higher levels of MUC2 immunopositivity was seen in HT29-MTX cells cultured in layers on alginate scaffolds compared to those suspended within alginate (Fig. 7A). Interestingly HT29-MTX cells cultured on or in L-pNIPAM hydrogel scaffolds showed some immunopositivity for MUC2 and a high

level of immunopositivity for MUC5AC (Fig. 7B). Whereas HT29-MTX cells layered on and suspended within L-pNIPAM-co-DMAc under static and dynamic culture conditions displayed weak immunopositivity for MUC2 with high immunopositivity for MUC5AC (Fig. 7C).

3.7. Scanning electron microscopy of HT29-MTX cells

SEM analysis of HT29-MTX cells suspended within and layered on L-pNIPAM and L-pNIPAM-co-DMAc hydrogel scaffolds under static and dynamic culture conditions at 21 days, showed the presence of cells within or on the surface of the hydrogel. Although HT29-MTX cells were suspended within L-pNIPAM and L-pNIPAM-co-DMAc hydrogel scaffolds, cells migrated to the surface of the hydrogels, where cells formed circular clusters of cells when cultured under static and dynamic culture conditions. It was found that the HT29-MTX cells layered on the hydrogels under both static and dynamic conditions, covered the hydrogels (Fig. 8A, B, and Supplementary Fig. 5).

4. Discussion

The human intestinal Caco-2 and HT29-MTX cells have been utilized as *in vitro* models of enterocytes and goblet cells, respectively [30]. Here, three hydrogel systems were investigated to determine which would support 3D culture of Caco-2 and HT29-MTX cells, and give rise to the villus architecture of the small intestine *in vitro*. Previous studies have reported the importance of culture conditions in the differentiation and functionality of cells [2,31,32]. Thus, here we compared cell behaviour in a softer alginate versus stiffer synthetic non-biodegradable scaffolds developed in our laboratory [26–28]; and compared cells cultured in suspension or as layers and maintained under static versus dynamic culture conditions.

569 Long-term static culture has been shown to contribute to decreased cell viability and
570 extracellular matrix production [32], thus, we utilized an orbital shaker as a simple
571 way to simulate dynamic culture conditions. This study showed that not only the
572 static or dynamic culture conditions impacted on the metabolic activity of Caco-2 and
573 HT29-MTX cells, but also the cellular localization within or on the three hydrogels
574 affected metabolic activity and tissue architecture.

575 To characterize the 3D culture models *in vitro*, metabolic activity of Caco-2 and
576 HT29-MTX cells were assessed within the three hydrogel scaffolds. The natural
577 biodegradable scaffold: calcium cross-linked alginate, maintained the metabolic
578 activity of Caco-2 and HT29-MTX cells for 21 days in some of the culture conditions
579 and induced formation of cell spheroids. In contrast, the metabolic activity was
580 decreased when Caco-2 cells were layered on alginate and cultured under dynamic
581 culture and when HT29-MTX cells were suspended within alginate and cultured
582 under static culture conditions. These differences between Caco-2 and HT29-MTX
583 cells may be attributed to differential expression or properties of cell receptors.
584 Simon-Assmann *et al* (1994) and Orian-Rousseau *et al* (1998), demonstrated that
585 Caco-2 and HT29-MTX cells produced different types of integrins, and that this could
586 affect how these cells grow in culture [33,34]. Simon-Assmann *et al* (1994) showed
587 that undifferentiated and differentiated HT29 cell populations cultured on laminin
588 produced different laminin-binding integrins and grew differently under identical
589 culture conditions [33]. These differences in integrins may in part explain the
590 difference in the growth seen in the HT29-MTX and Caco-2 cells observed in this
591 current study. In addition, the mechanical properties of alginate may also impact on
592 cell proliferation, differentiation, and morphological organisation [35]. The mechanical
593 properties of alginate are time dependent, the strength of alginate decreases

gradually during the first few weeks culture, due to the loss of calcium ions and the production of extracellular matrix by the cultured cells [36].

Taken together, the variable metabolic activity and spheroid morphology observed when Caco-2 and HT29-MTX cells were cultured in alginate, could in part be a result of the poor stability and changing properties seen in alginate; when used as a 3D scaffold in long term cell culture. Scaffold stability would be essential to maintain cells demanding stability and time to produce their own matrix [37], alginate was shown to have low storage moduli indicating a soft hydrogel and thus could have impacted on stability with time [38].

Caco-2 and HT29-MTX cells are sensitive to calcium and express the calcium sensing receptor [39,40] the main effects of calcium on these cells appear to be on cellular migration [41] and adhesion molecules [42]. Transepithelial electrical resistance (TEER) values increased in Caco-2 cells treated with 1.6mM Ca^{2+} for 1 hr [39]. However, within alginate cultures with the exception of the 10 minute polymerisation time, where cells are exposed within the alginate to 200mM $CaCl_2$, the Ca^{2+} is bound within the alginate as a cross linker as is not freely accessible to cells. During the preparation of alginate, following polymerisation the alginate is washed with NaCl and media, and media is changed every 48hrs, thus any remaining free Ca^{2+} would be rapidly removed. Chan *et al.,* (2013) demonstrated that in alginate which was unwashed following polymerisation 50% of the Ca^{2+} was released into the media over the first 10hrs [43]. Thus following the 3 weeks of culture in this study and extensive washes following polymerisation, limited free Ca^{2+} would be available for cellular uptake. In the bound form Ca^{2+} may be involved in activation of the Ca^{2+} sensing receptor but due to its bound form is unlikely to be

618 able to be taken up into cells and thus at the later time points of 2 and 3 weeks of
619 culture it is unlikely to have had a major effect on the cellular behaviour.

620 Here, we investigated the capacity of synthetic, non-biodegradable, non-fabricated,
621 cross-linked network structures which are highly hydrated and similar to the native
622 microenvironment of the small intestine to determine their ability to provide the
623 mechanical support for cellular proliferation and differentiation. Interestingly, the
624 phenotype of Caco-2 and HT29-MTX cells were similar in L-pNIPAM and L-pNIPAM-
625 co-DMAc. The metabolic activity of Caco-2 and HT29-MTX cells were increased
626 when layered on these hydrogels under both static and dynamic culture; with both
627 cell lines shown to form villus-like structures under dynamic culture. The observed
628 increases in metabolic activity and formation of the villus-like structure under
629 dynamic culture conditions, may be due to the flow of nutrients and oxygen over
630 cells, the fluid flow induced in these cultures will mimic the fluid flow of nutrients in
631 the small intestine. This efficient delivery of nutrients and oxygen enabled Caco-2
632 and HT29-MTX cells to reorganize into 3D villus-like structures that remained viable
633 for the 21 days investigated. Furthermore, these synthetic hydrogels also provided a
634 hydrated space for the diffusion of nutrients and metabolites to and from the Caco-2
635 and HT29-MTX cells. Thus stimulating the production of extracellular matrix (ECM)
636 and increasing cell adhesion. Caco-2 cells are known to increase cell-cell adhesion
637 through the production of E-cadherin-actin complexes [44], and shown to adhere to
638 decellularized scaffolds, and form villus-like structures when grown under dynamic
639 culture conditions [2].

640 In our synthetic hydrogel models, when Caco-2 cells were suspended within either L-
641 pNIPAM or L-pNIPAM-co-DMAc the metabolic activity of cells was reduced,
642 compared to alginate. It seems possible that these decreases in metabolic activity

643 were due to reduced nutrient diffusion through the synthetic hydrogels, this is
644 supported by the decreased pore size and increased stiffness seen in these
645 synthetic hydrogels. This finding, however is contrary to our previous study with
646 mesenchymal stem cells, which had excellent metabolic activity and cell
647 differentiation within L-pNIPAM-co-DMAc [28]. These differences in metabolic activity
648 within the hydrogel may reflect the relatively higher metabolic rate of the Caco-2 cells
649 compared to mesenchymal stem cells. This leads to the suggestion that Caco-2 cells
650 are more sensitive to reduced nutrient supply and/or diffusion of waste material when
651 suspended within either L-pNIPAM or L-pNIPAM-co-DMAc. In addition, there are
652 many parameters which can influence cell behaviour in 3D synthetic scaffolds such
653 as crosslinking density, porosity, and biodegradability [45]. Mechanical properties of
654 biomaterials have been shown previously to drive differentiation of cells. For
655 example, Baker *et al* (2009) found that the stiffness of the extracellular matrix plays
656 an important role in increasing the intracellular mechanical properties of prostate
657 cancer cells when mixed with different concentrations of type I collagen matrix [46].
658 Thus the differential stiffness seen within these systems could explain at least in part
659 the behaviour of cells within this study.

660 Mucins are an intrinsic part of the small intestinal niche, and these proteins give rise
661 to an adherent mucus layer that coat the intestinal mucosa [47]. Mucins provide
662 protection against pathogens and auto digestion, and act as a medium for digestion
663 and absorption [47,48]. *In vivo* MUC2 and MUC5AC mucins are secreted and gel-
664 forming mucin types and are expressed by intestinal cells to variable amounts [49–
665 51]. MUC2 is highly expressed in goblet cells of the small intestine and colon [52];
666 whereas MUC5AC is not normally expressed in the small and large intestinal
667 mucosa, and are mainly expressed in the stomach [50,51]. Within our hydrogel

models, immunohistochemical analysis showed that MUC2 and MUC5AC were not expressed by Caco-2 cells under any culture conditions. The expression of MUC5AC gene has been previously observed in Caco-2 cells, however this was measured by qRT-PCR and was not measured as protein production [52].

In the HT29-MTX cells, our results showed production of MUC2 and MUC5AC when cultured in and on L-pNIPAM or L-pNIPAM-co-DMAc under static or dynamic cultures. Our findings indicated a modification of predominantly MUC2 production to mostly MUC5AC in the HT29-MTX cells. This switching in mucin phenotype is common with formation of tumours and can be attributed to changes in the cell niche [47], thus the switching seen in the current study may be due to the fact that HT29-MTX cells are derived from human colon adenocarcinoma. During gastrointestinal cancers there is often an up-regulation of the more viscous and protective MUC5AC during disease progression especially were auto digestion can occur [53].

In this study, we have shown that the cell morphology varied dramatically between the three *in vitro* systems and indeed the native small intestinal epithelium. However, it was clear that the cell morphology was greatly influenced by the 3D microenvironment; with the presence of villus like structures being more common when cells were cultured on the surface of L-pNIPAM and L-pNIPAM-co-DMAc under dynamic culture conditions.

Immunohistochemical analysis showed the presence of CD10 and ZO-1 which confirmed the brush border and tight junction expression, respectively when Caco-2 cells were layered on L-pNIPAM under static and dynamic culture conditions. Despite the colonic origins of Caco-2 cells, when grown on L-pNIPAM they expressed small intestinal digestive enzymes sucrase-isomatlase, dipeptidyl

692 peptidase IV and alkaline phosphatase. Previous studies, have also shown
693 differentiation of Caco-2 cells into enterocyte-like cells, which mimic the cells of the
694 small intestine [15,54,55]. However, it is important to note that not all Caco-2 cells
695 produced sucrase-isomatlase, this may be due to the early passage of Caco-2 cells
696 used in this study. This patchy expression of sucrase-isomaltase has been shown to
697 vary in Caco-2 cells depending on the passage number [56]. Hence, we show that L-
698 pNIPAM not only stimulates Caco-2 differentiation in both culture conditions but also
699 maintained expression of enzymes which were expressed in monolayer. These
700 results propose a positive communication between the L-pNIPAM and the Caco-2
701 cells. These finding are in agreement with the previous studies which showed an
702 increase in alkaline phosphatase activity when Caco-2 cells grown as a monolayer
703 on polycarbonate filters [13] and when co-cultured with HT29-MTX cells on silk
704 scaffolds [57]. Similarly, Caco-2 cells cultured on the extracellular matrix proteins
705 (collagen type I and the basement membrane components collagen type IV and
706 laminin) also showed that the activity of alkaline phosphatase, dipeptidase II and
707 sucrase-isomaltase were significantly higher in cells grown on laminin or collagen
708 type IV than cells grown on collagen type I for one week after confluence as a result
709 of the effect of extracellular matrix proteins on the differentiation phenotype [55].

710 SEM analysis further confirmed Caco-2 differentiation when cultured in layers on L-
711 pNIPAM under static and dynamic culture conditions. The results revealed the typical
712 finger-like projections at the apical surface of Caco-2 cells layered on L-pNIPAM
713 suggesting differentiation and formation of microvilli. Caco-2 cells spread and
714 covered the surface of L-pNIPAM-co-DMAc under static and dynamic culture. It
715 seems possible that these differences in the morphological characteristics could be
716 due to differences in mechanical stiffness of these synthetic hydrogels [26,27].

This study, reports for the first time that synthetic non-biodegradable hydrogels could be used as scaffolds for Caco-2 and HT29-MTX cells. The most effective scaffold which supported both cell lines and induced the formation of the optimal villus like structures was L-pNIPAM when cells were layered on the surface and cultured under dynamic conditions. Despite these promising findings, future work is required to investigate the capacity of the L-pNIPAM as a scaffold to co-culture Caco-2 and HT29-MTX cells under dynamic culture conditions to develop a 3D model of the small intestinal epithelium.

5. Conclusion

Here, we have shown that Caco-2 and HT29-MTX cells were successfully layered on L-pNIPAM hydrogel scaffolds under dynamic culture conditions which supported the 3D culture of these cells and stimulated them to form villus-like structures, maintained differentiation into enterocyte-like cells and mucus-producing goblet cells, respectively which expressed phenotypic markers that mimicked the native small intestinal epithelium. Thus, L-pNIPAM has the potential to deliver a 3D culture of Caco-2 and HT29-MTX cells which is promising for further investigation and characterisation of 3D *in vitro* co-culture model which could be used in drug discovery, and studies investigating inflammatory bowel disease and used as an alternative to *in vivo* animal models in drug toxicity studies.

6. Author contributions

RHD performed the majority of the laboratory work, data analysis and statistical analysis, contributed to study design and drafted the manuscript. AE performed the DMA and pore size analysis and associated statistical analysis, contributed to study design and critically revised the manuscript. NJM, CS, and CLLM conceived the

study, participated in its design and analysis and critically revised the manuscript. All authors read and approved the final manuscript.

7. Acknowledgments

This work was funding by Ministry of Higher Education and Scientific Research / Iraq and Libyan Ministry of Higher Education for the PhD scholarships. The authors thank Mr. J Roe for his assistance in SEM.

Figure Legends:

Figure 1: Viability of Caco-2 cells at a cell density of 2×10^6 cells/ml layered on or suspended within alginate: A, B, C, D; L-pNIPAM: E, F, G, H; L-pNIPAM-co-DMAc: I, J, K, L following 21 days under static and dynamic culture conditions .*$p = \leq 0.05$.

Figure 2: Histological analysis of Caco-2 cells layered on or suspended within alginate, L-pNIPAM, and L-pNIPAM-co-DMAc hydrogels under static or dynamic culture conditions at a cell density of 2×10^6 cells/ml following 21 days. A: stained with H&E (circles indicate villus like structures) and B: stained with Alcian blue/PAS, blue: acidic mucin (black arrows); magenta: neutral mucin (red arrows). *Scale bar = 100µm*.

Figure 3: Immunohistochemistry staining (brown) for CD10, ZO-1, Alkaline phosphatase (ALP), Dipeptidyl peptidase IV (DPP IV), and Sucrase-isomaltase (SI) of Caco-2 cells in 0h monolayer and Caco-2 cells layered on L-pNIPAM under static or dynamic culture conditions at a cell density of 2×10^6 cells/ml following 21 day. Cell nuclei were stained with haematoxylin (blue). Yellow arrows indicate positively stained cells. IgGs as a negative control. *Scale bar = 100µm*.

Figure 4: Scanning electron microscopy of Caco-2 cells layered on A: L-pNIPAM-; B: L-pNIPAM-co-DMAc hydrogels under static or dynamic culture conditions at a cell density of 2×10^6 cells/ml following 21 days. White arrows indicate microvilli structures. *Scale bar = 200µm, 30µm, or 100µm, 50µm.*

Figure 5: Viability of HT29-MTX cells at a cell density of 2×10^6 cells/ml layered on or suspended within alginate: A, B, C, D; L-pNIPAM: E, F, G, H; L-pNIPAM-co-DMAc: I,J,K,L following 21 days under static or dynamic culture conditions .*$p = \leq 0.05$.

Figure 6: Histological analysis of HT29-MTX cells layered on or suspended within alginate, L-pNIPAM, and L-pNIPAM-co-DMAc hydrogels under static or dynamic culture conditions at a cell density of 2×10^6 cells/ml following 21 days. A: stained with H&E (circles indicate villus like structures) and B: stained with Alcian blue/PAS, blue: acidic mucin (black arrows); magenta: neutral mucin (red arrows). *Scale bar = 100µm.*

Figure 7: Immunohistochemistry staining (brown) of MUC2 and MUC5AC; A: monolayer and IgG as a negative control. HT29-MTX cells layered on or suspended within B: alginate, C: L-pNIPAM, and D: L-pNIPAM-co-DMAc hydrogels under static or dynamic culture conditions at a cell density of 2×10^6 cells/ml following 21 days. Cell nuclei were stained with haematoxylin (blue). Yellow arrows indicate positively stained cells. *Scale bar = 100µm*.

Figure 8: Scanning electron micrographs of HT29-MTX cells layered on or suspended within A: L-pNIPAM and B: L-pNIPAM-co-DMAc hydrogels under static or dynamic culture conditions at a cell density of 2×10^6 cells/ml following 21 days. White circles indicate clusters of cells. *Scale bar A = 200µm or 30µm; B= 100µm or 50µm*.

References

[1] C.M. Costello, J. Hongpeng, S. Shaffiey, J. Yu, N.K. Jain, D. Hackam, J.C. March, Synthetic small intestinal scaffolds for improved studies of intestinal differentiation, Biotechnol. Bioeng. 111 (2014) 1222–1232.

[2] J. Pusch, M. Votteler, S. Göhler, J. Engl, M. Hampel, H. Walles, K. Schenke-Layland, The physiological performance of a three-dimensional model that mimics the microenvironment of the small intestine, Biomaterials. 32 (2011) 7469–7478.

[3] M. Ravi, V. Paramesh, S.R. Kaviya, E. Anuradha, F.D. Solomon, 3D Cell Culture Systems: Advantages and Applications, J. Cell. Physiol. 230 (2015) 16–26.

[4] F. Pampaloni, E.H.K. Stelzer, A. Masotti, Three-dimensional tissue models for drug discovery and toxicology, Recent Pat. Biotechnol. 3 (2009) 103–117.

[5] F. Pampaloni, E.G. Reynaud, E.H.K. Stelzer, The third dimension bridges the gap between cell culture and live tissue., Nat. Rev. Mol. Cell Biol. 8 (2007) 839–845.

[6] C. Pontier, J. Pachot, R. Botham, B. Lenfant, P. Arnaud, HT29-MTX and Caco-2/TC7 monolayers as predictive models for human intestinal absorption: Role of the mucus layer, J. Pharm. Sci. 90 (2001) 1608–1619.

[7] Y. Imura, Y. Asano, K. Sato, E. Yoshimura, A microfluidic system to evaluate intestinal absorption, Anal. Sci. 25 (2009) 1403–1407.

[8] J.H. Sung, J. Yu, D. Luo, M.L. Shuler, J.C. March, Microscale 3-D hydrogel scaffold for biomimetic gastrointestinal (GI) tract model, Lab Chip. 11 (2011) 389–392.

[9] H.J. Kim, D.E. Ingber, Gut-on-a-Chip microenvironment induces human

intestinal cells to undergo villus differentiation, Integr. Biol. 5 (2013) 1130.

[10] A.L. Kauffman, A. V. Gyurdieva, J.R. Mabus, C. Ferguson, Z. Yan, P.J. Hornby, Alternative functional in vitro models of human intestinal epithelia, Front. Pharmacol. 4 (2013) 1–18.

[11] T. Yoshikawa, S. Hamada, E. Otsuji, H. Tsujimoto, A. Hagiwara, Endocrine differentiation of rat enterocytes in long-term three-dimensional co-culture with intestinal myofibroblasts, Vitr. Cell. Dev. Biol. 47 (2011) 707–715.

[12] M.E. Viney, A.J. Bullock, M.J. Day, S. MacNeil, The co-culture of intestinal epithelial and stromal cells in 3D collagen-based environments, Regen. Med. 4 (2009) 397–406.

[13] S. Ferruzza, C. Rossi, M.L. Scarino, Y. Sambuy, A protocol for in situ enzyme assays to assess the differentiation of human intestinal Caco-2 cells, Toxicol. Vitr. 26 (2012) 1247–1251.

[14] S. Howell, A.J. Kenny, A.J. Turner, A survey of membrane peptidases in two human colonic cell lines, Caco-2 and HT-29., Biochem. J. 284 (1992) 595–601.

[15] O. Anna, L. Monika, G. Wodzimierz, C. Katarzyna, New rapid method of Caco-2 cell differentiation, Polish J. Food Nutr. Sci. 12 (2003) 60–64.

[16] H. Sung, E.C. Chow, S. Liu, Y. Du, K.S. Pang, The Caco-2 cell monolayer: usefulness and limitations, Expert Opin. Drug Metab. Toxicol. 4 (2008) 395–411.

[17] M. Natoli, B.D. Leoni, I. D'agnano, M. D'onofrio, R. Brandi, I. Arisi, F. Zucco, A. Felsani, Cell growing density affects the structural and functional properties of Caco-2 differentiated monolayer, J. Cell. Physiol. 226 (2011) 1531–1543. doi:10.1002/jcp.22487.

[18] M. Gagnon, A. Zihler Berner, N. Chervet, C. Chassard, C. Lacroix, Comparison of the Caco-2, HT-29 and the mucus-secreting HT29-MTX intestinal cell models to investigate Salmonella adhesion and invasion, J. Microbiol. Methods. 94 (2013) 274–279.

[19] C.M. Costello, R.M. Sorna, Y. Goh, I. Cengic, N.K. Jain, J.C. March, 3‐D Intestinal Scaffolds for Evaluating the Therapeutic Potential of Probiotics, Mol. Pharm. 11 (2014) 2030–2039.

[20] J. Yu, S. Peng, D. Luo, J.C. March, In vitro 3D human small intestinal villous model for drug permeability determination., Biotechnol. Bioeng. 109 (2012) 2173–8.

[21] S.H. Kim, M. Chi, B. Yi, S.H. Kim, S. Oh, Y. Kim, S. Park, J.H. Sung, Three Dimentional intestinal villi epithelium enhances protection of human intestinal cells from bacterial infection by inducing mucin, Integr. Biol. 6 (2014) 1122–1131.

[22] J.H. Sung, J. Yu, D. Luo, M.L. Shuler, J.C. March, Microscale 3-D hydrogel scaffold for biomimetic gastrointestinal (GI) tract model, Lab Chip. 11 (2011) 389–392.

[23] L. Wu, J. Ding, In vitro degradation of three-dimensional porous poly (D, L-lactide-co-glycolide) scaffolds for tissue engineering, Biomaterials. 25 (2004) 5821–5830.

[24] W.R. Gombotz, S. Wee, Protein release from alginate matrixes, Adv. Drug Deliv. Rev. 31 (1998) 267–285.

[25] A. Khavari, M. Nydén, D.A. Weitz, A.J. Ehrlicher, Composite alginate gels for tunable cellular microenvironment mechanics, Sci. Rep. 6 (2016) 1–10.

[26] V. Boyes, C. Sammon, C. Le Maitre, C. Breen, The Synthesis and

Development of Novel , Easily Processable Poly (N- Isopropylacrylamide) - Based Hydrogels, Sheffield Hallam University. Faculty of Arts, Computing, Engineering and Sciences, 2012. doi:Thesis no. 27578.

[27] V. Boyes, C. Sammon, C. Le Maitre, C. Breen, Composite hydrogel-clay particles. Patent, i.d:WO2013027051A1, 2013.

[28] A.A. Thorpe, V.L. Boyes, C. Sammon, C.L. Le Maitre, Thermally triggered injectable hydrogel, which induces mesenchymal stem cell differentiation to nucleus pulposus cells: Potential for regeneration of the intervertebral disc, Acta Biomater. 36 (2016) 99–111.

[29] C.L. Le Maitre, A.J. Freemont, J.A. Hoyland, The role of interleukin-1 in the pathogenesis of human intervertebral disc degeneration., Arthritis Res. Ther. 7 (2005) R732–R745.

[30] X.M. Chen, I. Elisia, D.D. Kitts, Defining conditions for the co-culture of Caco-2 and HT29-MTX cells using Taguchi design, J. Pharmacol. Toxicol. Methods. 61 (2010) 334–342. doi:10.1016/j.vascn.2010.02.004.

[31] N. Li, D. Wang, Z. Sui, X. Qi, L. Ji, X. Wang, L. Yang, Development of an improved three-dimensional in vitro intestinal mucosa model for drug absorption evaluation, Tissue Eng. Part C Methods. 19 (2013) 708–719.

[32] M.J. Jaasma, N.A. Plunkett, F.J. O'Brien, Design and validation of a dynamic flow perfusion bioreactor for use with compliant tissue engineering scaffolds, J. Biotechnol. 133 (2008) 490–496.

[33] P. Simon-Assmann, C. Leberquier, N. Molto, T. Uezato, F. Bouziges, M. Kedinger, Adhesive properties and integrin expression profiles of two colonic cancer populations differing by their spreading on laminin, J Cell Sci. 107 (1994) 577–587.

[34] V. Orian-Rousseau, D. Aberdam, P. Rousselle, A. Messent, J. Gavrilovic, G. Meneguzzi, M. Kedinger, P. Simon-Assmann, Human colonic cancer cells synthesize and adhere to laminin-5. Their adhesion to laminin-5 involves multiple receptors among which is integrin alpha2beta1., J. Cell Sci. 111 (1998) 1993–2004.

[35] S.R. Akhilesh Banerjee, Manish Arha, Soumitra Choudhary, Randolph S. Ashton, and R.S.K. Bhatia, David V. Schaffer, The Influence of Hydrogel Modulus on the Proliferation and Differentiation of Encapsulated Neural Stem Cells, Biomaterials. 30 (2009) 4695–4699.

[36] M.A. LeRoux, F. Guilak, L.A. Setton, Compressive and shear properties of alginate gel: Effects of sodium ions and alginate concentration, J. Biomed. Mater. Res. 47 (1999) 46–53.

[37] H.J. Wang, L. Di, Q.S. Ren, J.Y. Wang, Applications and degradation of proteins used as tissue engineering materials, Materials (Basel). 2 (2009) 613–635.

[38] M.S. Shoichet, R.H. Li, M.L. White, S.R. Winn, Stability of hydrogels used in cell encapsulation: An in vitro comparison of alginate and agarose, Biotechnol. Bioeng. 50 (1996) 374–381.

[39] S.L. Davies, C.E. Gibbons, M.C. Steward, D.T. Ward, Extracellular calcium- and magnesium-mediated regulation of passive calcium transport across Caco-2 monolayers, Biochim. Biophys. Acta. 1778 (2008) 2318–2324.

[40] L. Poquet, M.N. Clifford, G. Williamson, Transport and Metabolism of Ferulic Acid through the Colonic Epithelium, Am. Soc. Pharmacol. Exp. Ther. 36 (2008) 190–197.

[41] G. Peignon, S. Thenet, C. Schreider, S. Fouquet, A. Ribeiro, E. Dussaulx, J.

Chambaz, P. Cardot, M. Pinçon-Raymond, J. Le Beyec, E-cadherin-dependent transcriptional control of apolipoprotein A-IV gene expression in intestinal epithelial cells, J. Biol. Chem. 281 (2006) 3560–3568.

[42] M.F. Bernet, D. Brassart, J.R. Neeser, A.L. Servin, Adhesion of human bifidobacterial strains to cultured human intestinal epithelial cells and inhibition of enteropathogen-cell interactions, Appl. Environ. Microbiol. 59 (1993) 4121–4128.

[43] G. Chan, D.J. Mooney, Ca2+ released from calcium alginate gels can promote inflammatory responses in vitro and in vivo, Acta Biomater. 9 (2013) 9281–9291.

[44] C. Schreider, G. Peignon, S. Thenet, J. Chambaz, M. Pinçon-Raymond, Integrin-mediated functional polarization of Caco-2 cells through E-cadherin--actin complexes., J. Cell Sci. 115 (2002) 543–552.

[45] J.L. Drury, D.J. Mooney, Hydrogels for tissue engineering: scaffold design variables and applications, Biomaterials. 24 (2003) 4337–4351.

[46] E.L. Baker, R.T. Bonnecaze, M.H. Zaman, Extracellular matrix stiffness and architecture govern intracellular rheology in cancer, Biophys. J. 97 (2009) 1013–1021.

[47] H. Kitamura, M. Cho, B.H. Lee, J.R. Gum, B.B. Siddiki, S.B. Ho, N.W. Toribara, T. Lesuffleur, A. Zweibaum, Y. Kitamura, S. Yonezawa, Y.S. Kim, Alteration in mucin gene expression and biological properties of HT29 colon cancer cell subpopulations, Eur. J. Cancer. 32A (1996) 1788–1796.

[48] D.M. Moncada, S.J. Kammanadiminti, K. Chadee, Mucin and Toll-like receptors in host defense against intestinal parasites, Trends Parasitol. 19 (2003) 305–311.

946 [49] Y.S. Kim, S.B. Ho, Intestinal goblet cells and mucins in health and disease:
947 Recent insights and progress, Curr. Gastroenterol. Rep. 12 (2010) 319–330.
948 [50] Y.S. Kim, J.R. Gum, Diversity of mucin genes, structure, function, and
949 expression, Gastroenterology. 109 (1995) 999–1001.
950 [51] X.D. Bu, N. Li, X.Q. Tian, L. Li, J.S. Wang, X.J. Yu, P.L. Huang, Altered
951 expression of MUC2 and MUC5AC in progression of colorectal carcinoma,
952 World J. Gastroenterol. 16 (2010) 4089–4094.
953 [52] X.D. Bu, N. Li, X.Q. Tian, P.L. Huang, Caco-2 and LS174T cell lines provide
954 different models for studying mucin expression in colon cancer, Tissue Cell. 43
955 (2011) 201–206. doi:10.1016/j.tice.2011.03.002.
956 [53] L.Y.M. Wan, K.J. Allen, P.C. Turner, H. El-nezami, Modulation of mucin mRNA
957 (MUC5AC AND MUC5B) expression and protein production and secretion in
958 Caco-2/HT29-MTX Co-cultures following exposure to individual and combined
959 Fusarium mycotoxins, Toxicol. Sci. 139 (2014) 83–98.
960 [54] C. Jumarie, C., Malo, Caco-2 cells cultured in serum-free medium as a model
961 for the study of enterocytic differentiation in vitro, J. Cell. Physiol. 149 (1991)
962 24–33.
963 [55] M.D. Basson, G. Turowski, N.J. Emenaker, Regulation of Human (Caco-2)
964 Intestinal Epithelial Cell Differentiation by Extracellular Matrix Proteins, Exp.
965 Cell Res. 225 (1996) 301–305.
966 [56] I. Chantret, A. Rodolosse, A. Barbat, E. Dussaulx, E. Brot-Laroche, A.
967 Zweibaum, M. Rousset, Differential expression of sucrase-isomaltase in clones
968 isolated from early and late passages of the cell line Caco-2: evidence for
969 glucose-dependent negative regulation., J. Cell Sci. 107 (1994) 213–225.
970 [57] Y. Chen, Y. Lin, K.M. Davis, Q. Wang, J. Rnjak-kovacina, C. Li, R.R. Isberg,

C.A. Kumamoto, J. Mecsas, D.L. Kaplan, Robust bioengineered 3D functional human intestinal epithelium, Sci. Rep. 5 (2015) 1–11.

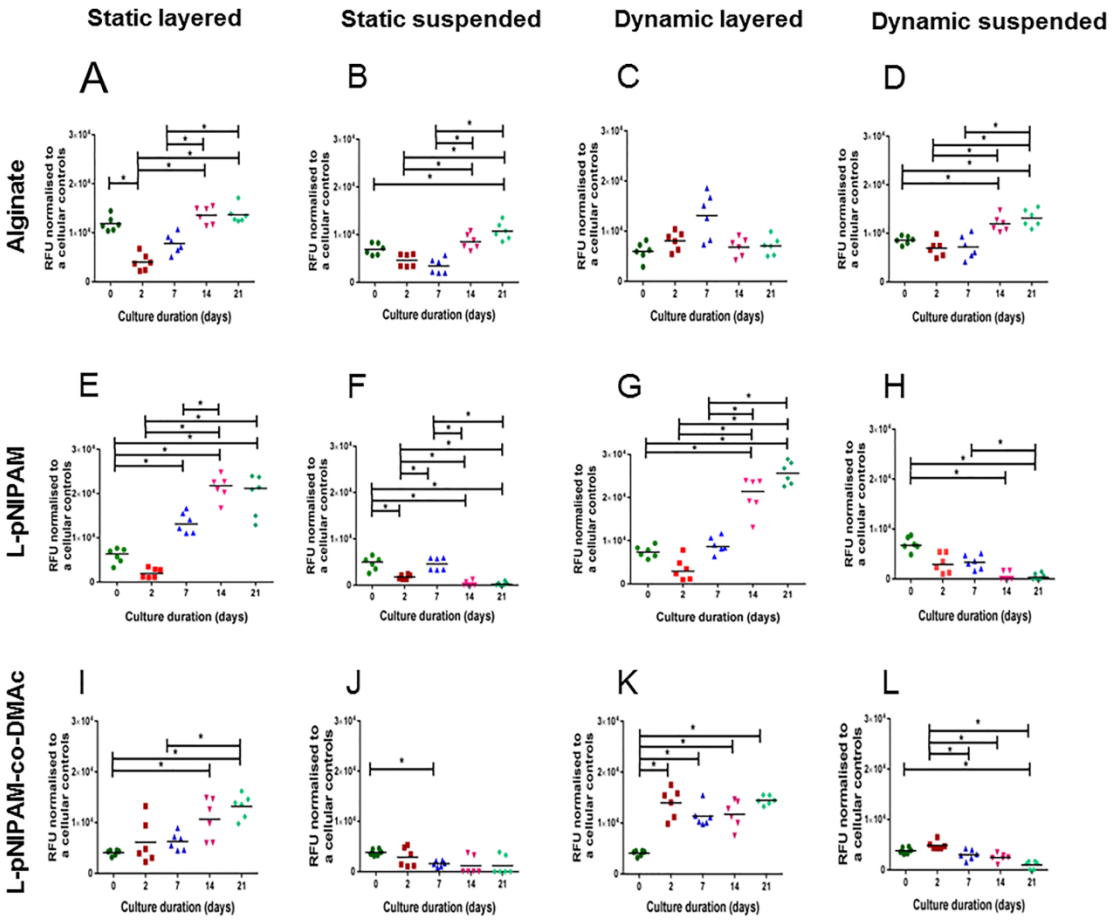

975

976 **Figure 1**

977

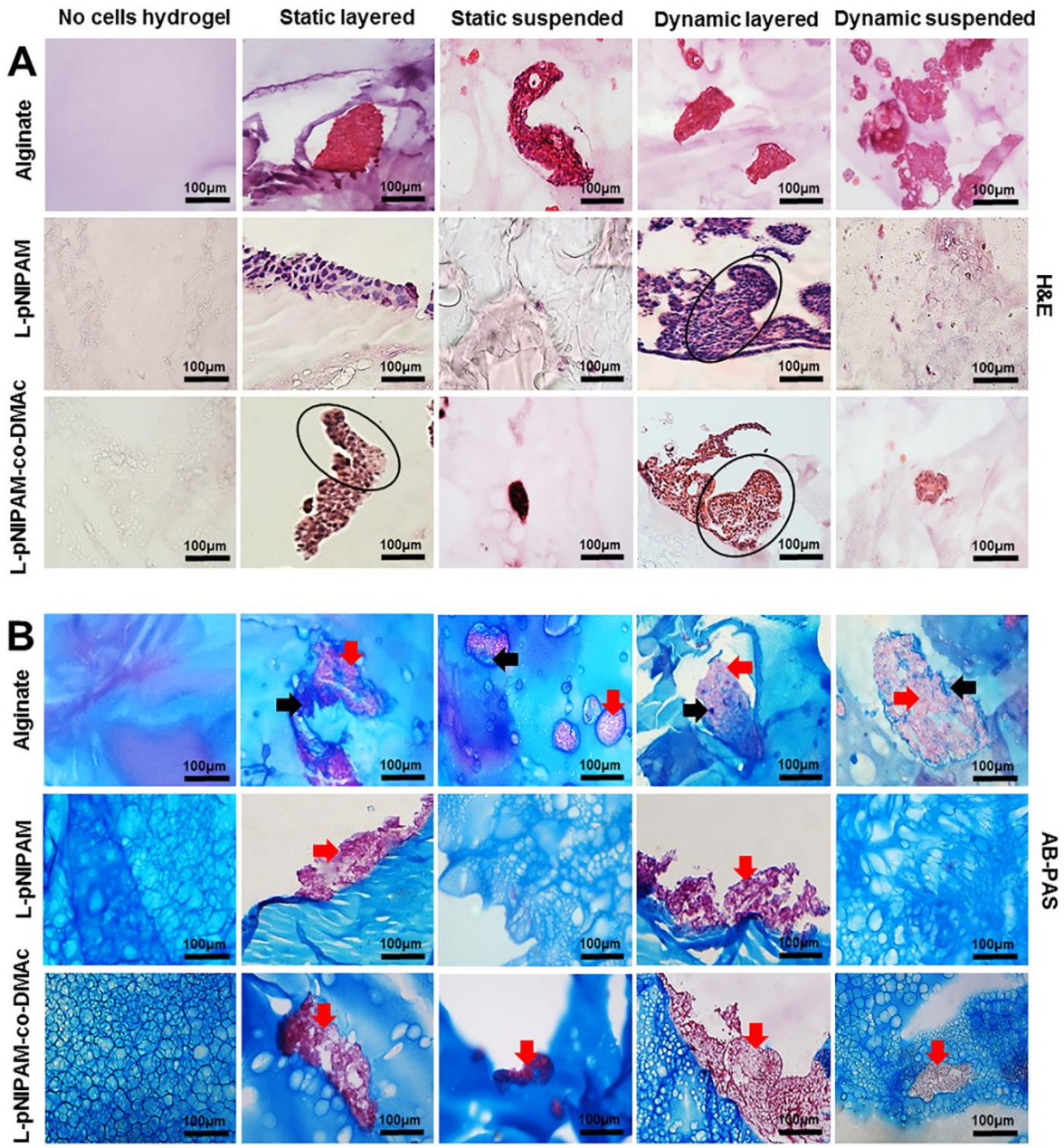

978

979 **Figure 2**

980

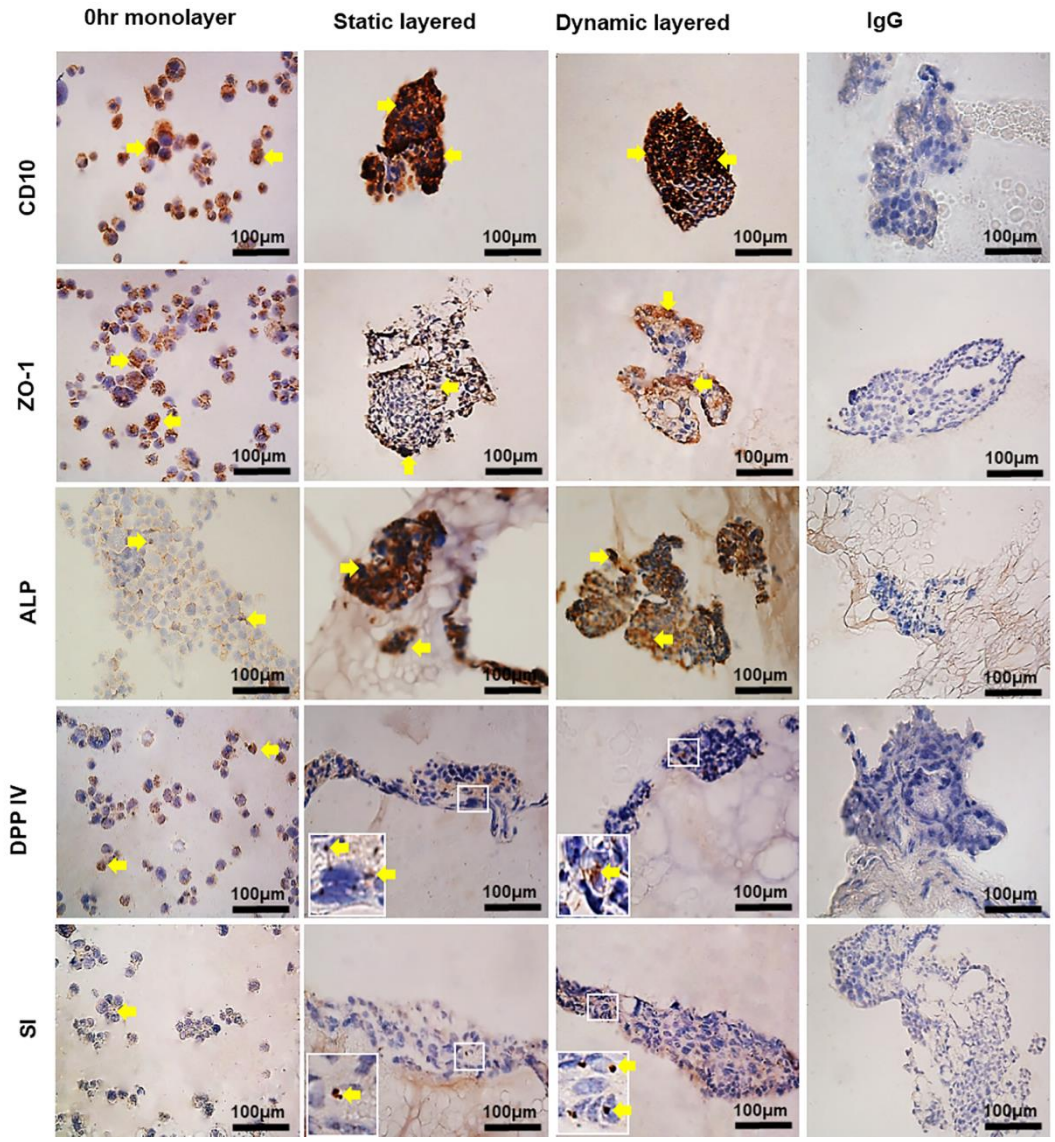

981

982 **Figure 3**

983

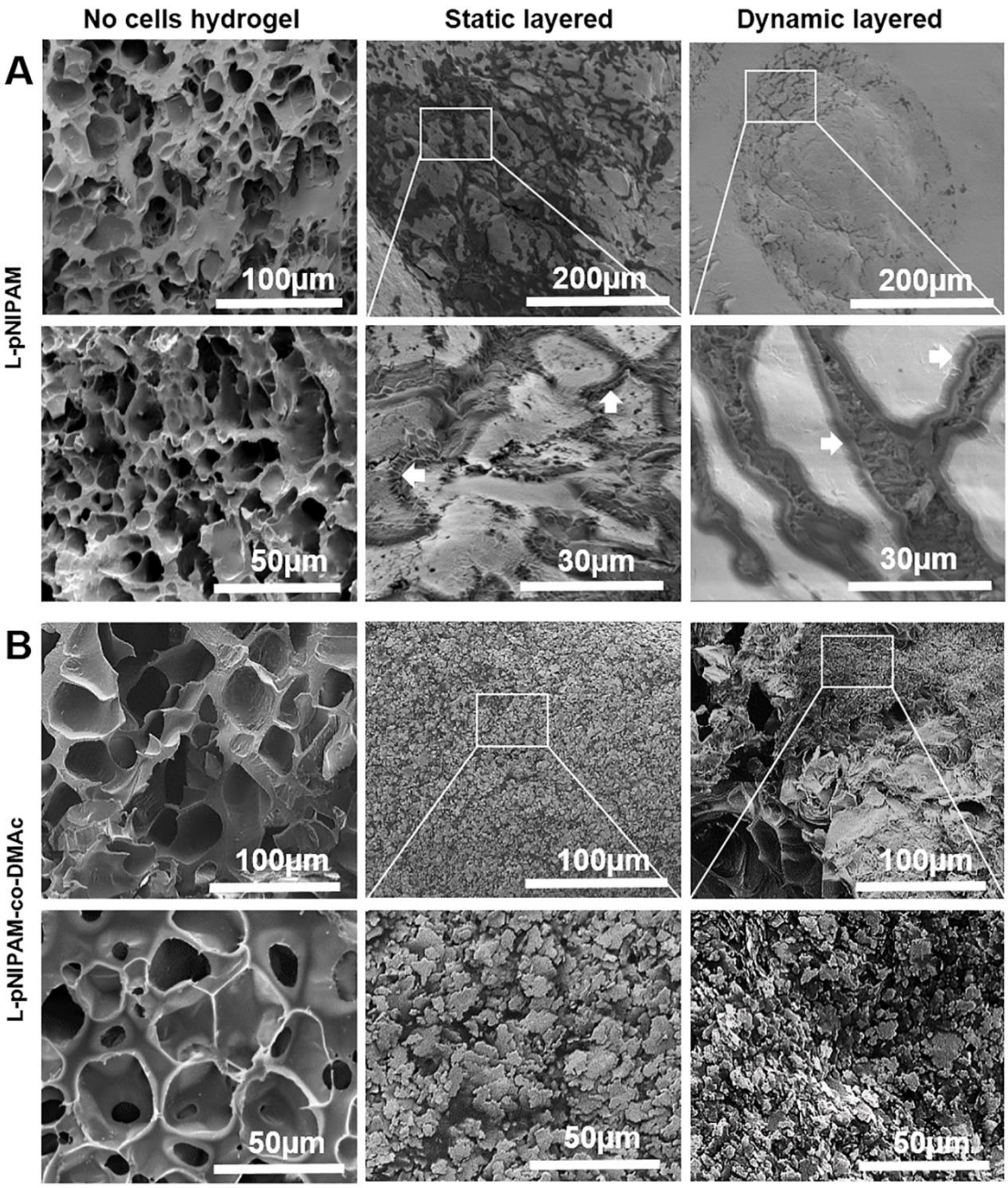

984

985 **Figure 4**

986

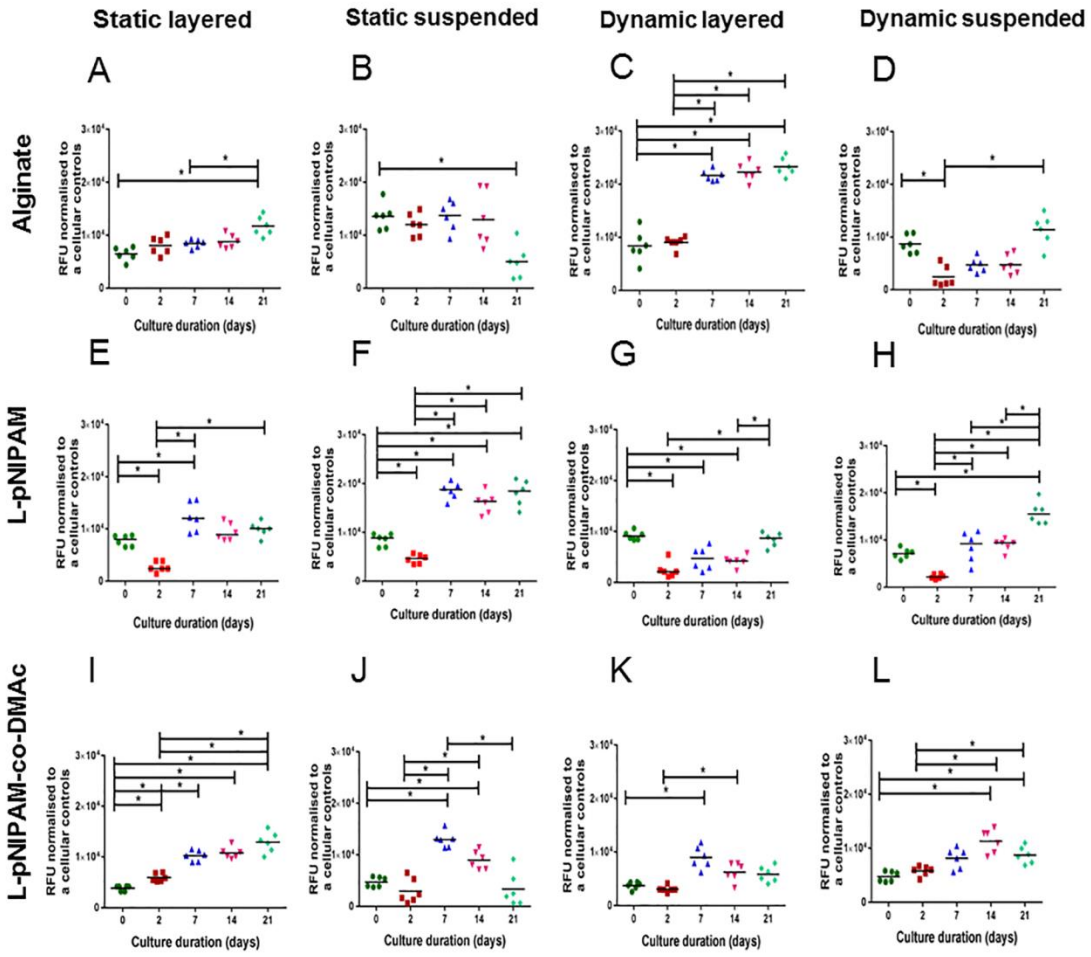
Static layered
Static suspended
Dynamic layered
Dynamic suspended
A
B
C
D
E
F
G
H
I
J
K
L
Alginate
L-pNIPAM
L-pNIPAM-co-DMAc
RFU normalised to a cellular controls
Culture duration (days)

Figure 5

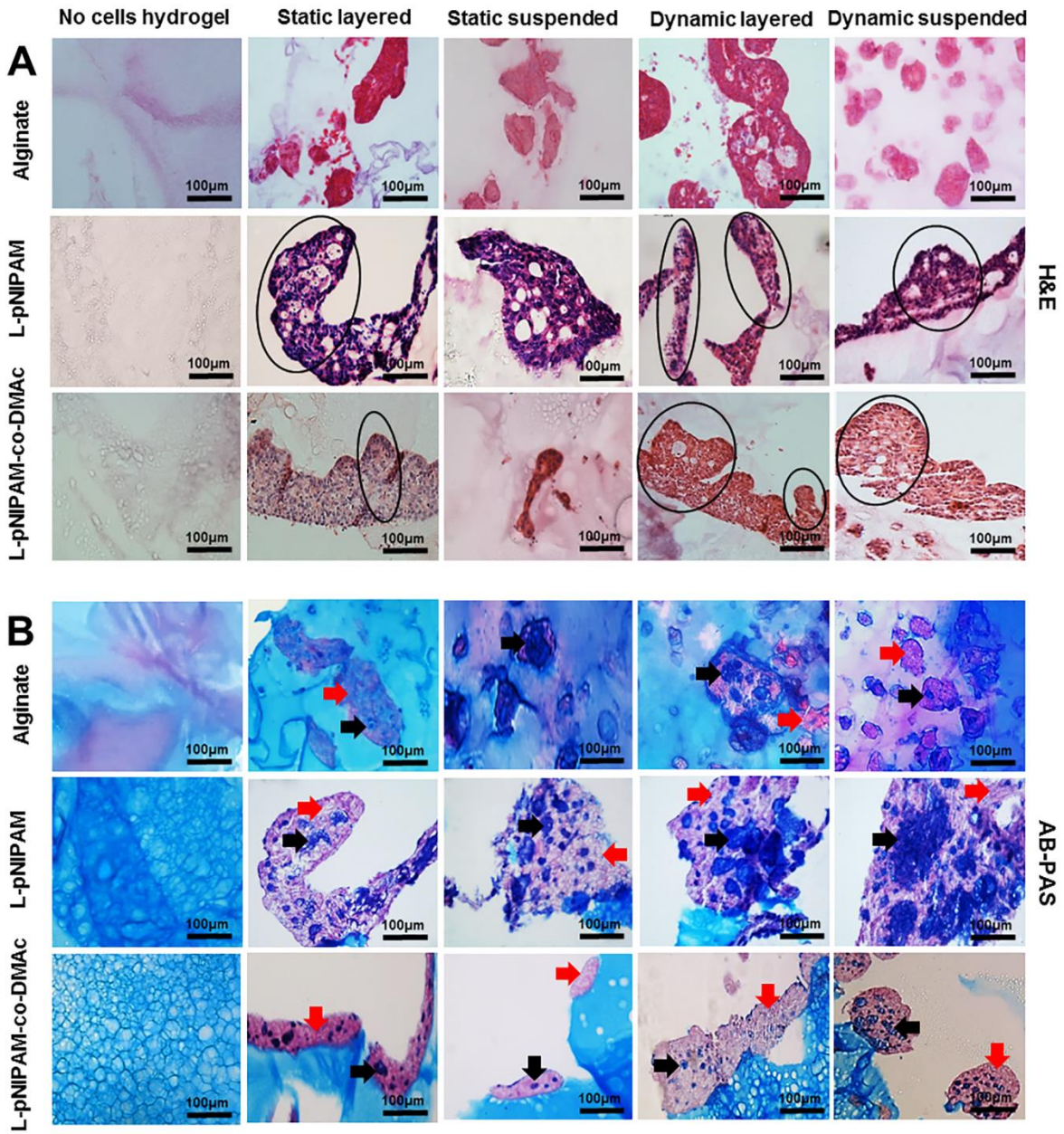

990

991 **Figure 6**

992

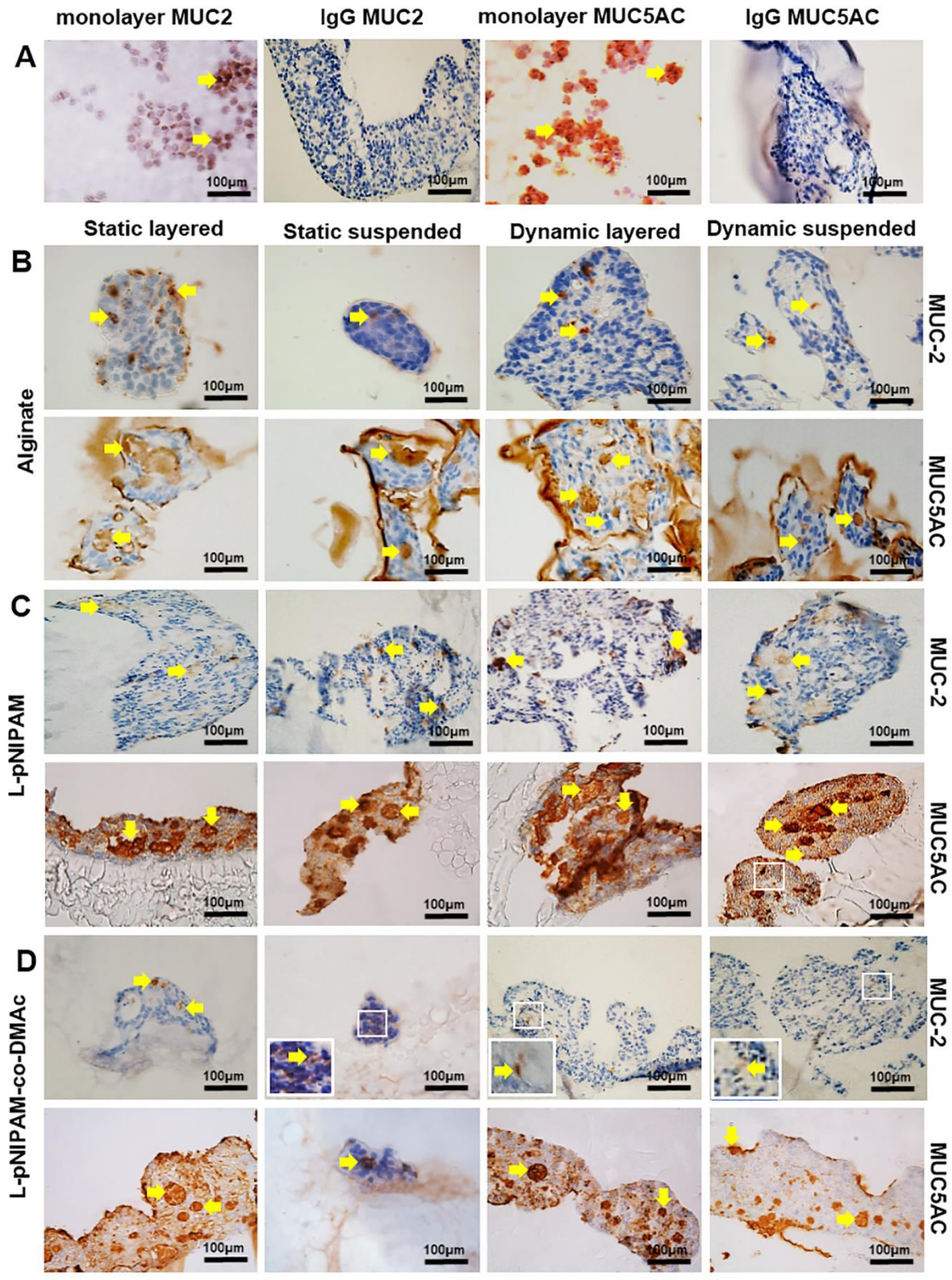

993

994 **Figure 7**

995

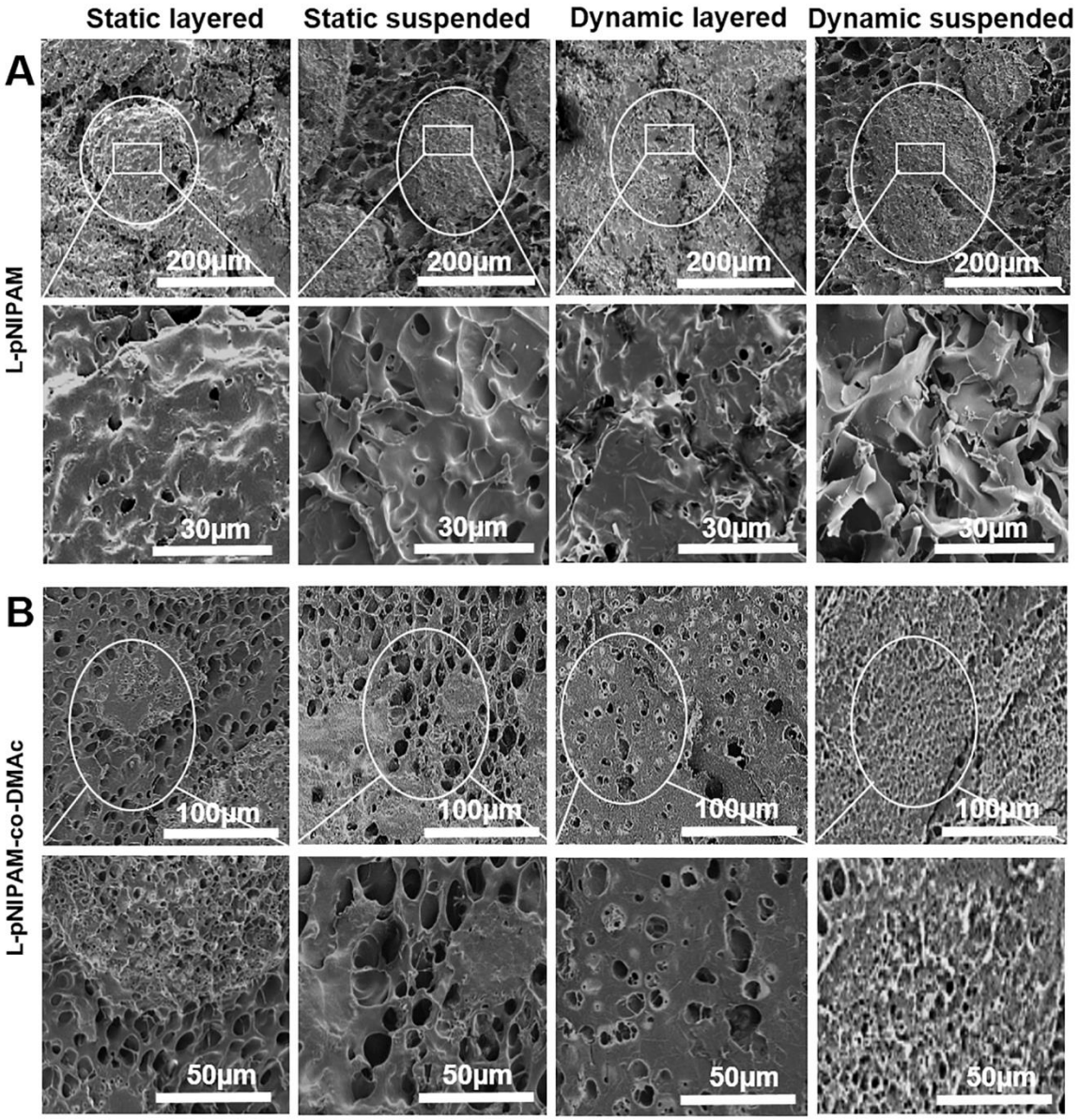

996

997 **Figure 8**

998

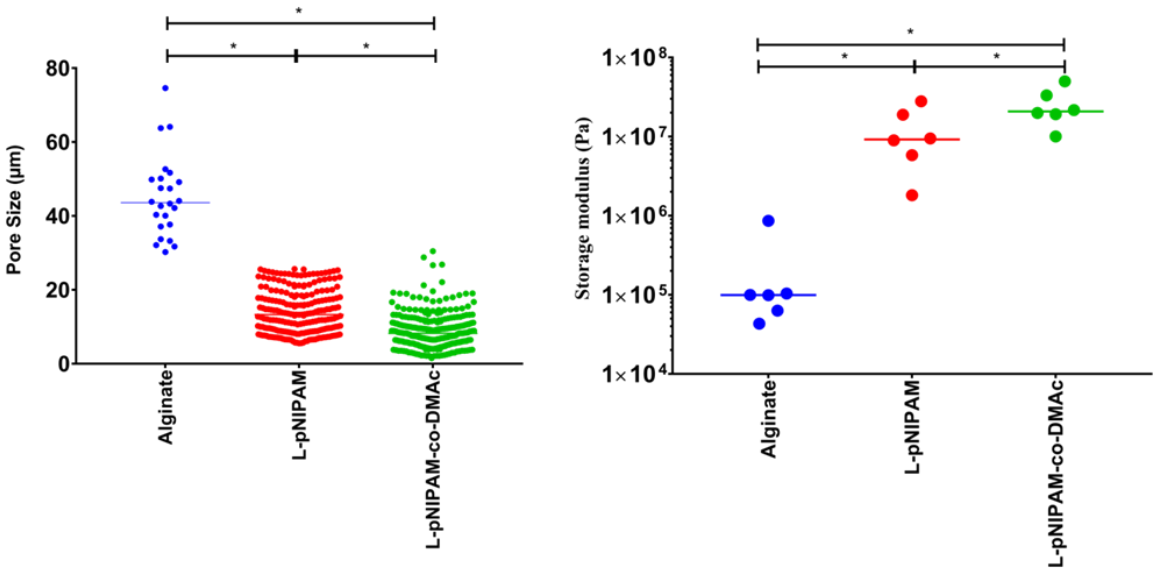

Supplementary Fig. 1. A: Pore size (µm) for acellular alginate, L-pNIPAM, and L-pNIPAM-co-DMAc hydrogels determined using SEM analysis. B: Storage Modulus (G') values for acellular alginate, L-pNIPAM, and L-pNIPAM-co-DMAc hydrogels determined using DMA.